Electronic Supplementary Material (ESI) for Journal of Materials Chemistry C.

The Spin Filtering of a Termination-controlled LSMO/Alq_3 heterojunction for an Organic Spin Valve

Tu-Ngoc Lam [1,2], Yen-Lin Huang[2], Ke-Chuan Weng[3], Yu-Ling Lai[1], Ming-Wei Lin[1], Ying-Hao Chu[2], Hong-Ji Lin[1], Chao-Cheng Kaun[3], Der-Hsin Wei[1], Yuan-Chieh Tseng[2,*], and Yao-Jane Hsu[1,4,*]

[1]*National Synchrotron Radiation Research Center, 101 Hsin-Ann Road, Hsinchu Science Park, Hsinchu, 30076, Taiwan, ROC*

[2]*Department of Materials Science and Engineering, National Chiao Tung University, Hsinchu, 30010, Taiwan, ROC*

[3]*Research Center for Applied Sciences, Academia Sinica, 128 Sec. 2, Academia Road, Nankang, Taipei 11529, Taiwan, ROC*

[4] *Department of Photonics, National Cheng Kung University, Tainan 70101, Taiwan, R.O.C.*

* Electronic mail: yjhsu@nsrrc.org.tw

* Electronic mail: ycsteng21@mail.nctu.edu.tw

The successful growth of terminated layers was verified with AFM images that exhibit the well-defined atomic control of formation layer by layer at the surface of MnO_2 and LSO terminations, seen in Fig. S1.

A mode of growth layer by layer was demonstrated with RHEED through a clear intensity of the oscillations during the fabrication of LSMO termination layers, as illustrated in Fig. S2. The MnO_2-ter was attained on growing directly LSMO (50 u. c.) on the TiO_2-terminated STO substrate. To achieve the LSO-ter, the STO substrate was switched from the TiO_2 termination to the SrO termination on inserting a thin layer (2.5 u. c.) of SRO and STO (15 u. c.) was then deposited, which was followed by the subsequent deposition of LSMO (50 u. c.).

The spectra of Mn $2p_{3/2}$ were deconvoluted into Mn^{3+} and Mn^{4+} with their binding energies (BE) 641.3 eV and 643.0 eV [1] for LSMO films of all three kinds, shown in Fig. S3. The intensity ratio Mn^{3+}:Mn^{4+} is 0.7:0.3, which agrees well with the stoichiometry ratio of the bulk perovskite $La_{0.7}Sr_{0.3}MnO_3$. Moreover, the Mn^{3+}:Mn^{4+} intensity ratio remains unchanged with take-off angle dependence, indicating the existence of two valence states of Mn at the surface of all LSMO films. In Fig. S4, the La 4d spectra were deconvoluted into two components, namely one doublet and one singlet with their relative BE the same for LSMO of all three kinds. These two components were separated by 2.8 eV and had unequal peak widths [2-3]. Similar to Mn 2p XPS spectra, the intensity ratio of the doublet and singlet does not change significantly with varying take-off angles; two components observed in La 4d thus reveal no difference in both bulk and surface information.

In Sr 3d and O 1s XPS, the relative ratio between the lower BE and the higher BE doublet greatly increased at the normal emission, attesting the assignment of bulk and surface components in our work, presented in Tables 1 and 2.

The molecular states of bulk Alq_3 at HOMO, HOMO+1, HOMO+2, HOMO+3, HOMO+4, HOMO+5 were stated at BE 2.6, 3.9, 5.0, 7.2, 9.5 and 11.4 eV in Fig. S5(a) and (d). The work functions of mixed and MnO_2 terminations were 4.4 and 4.5 eV; they decreased by the same value

0.5 eV after multilayer Alq_3 adsorption, shown in Fig. S5(b), (c), (e), and (f).

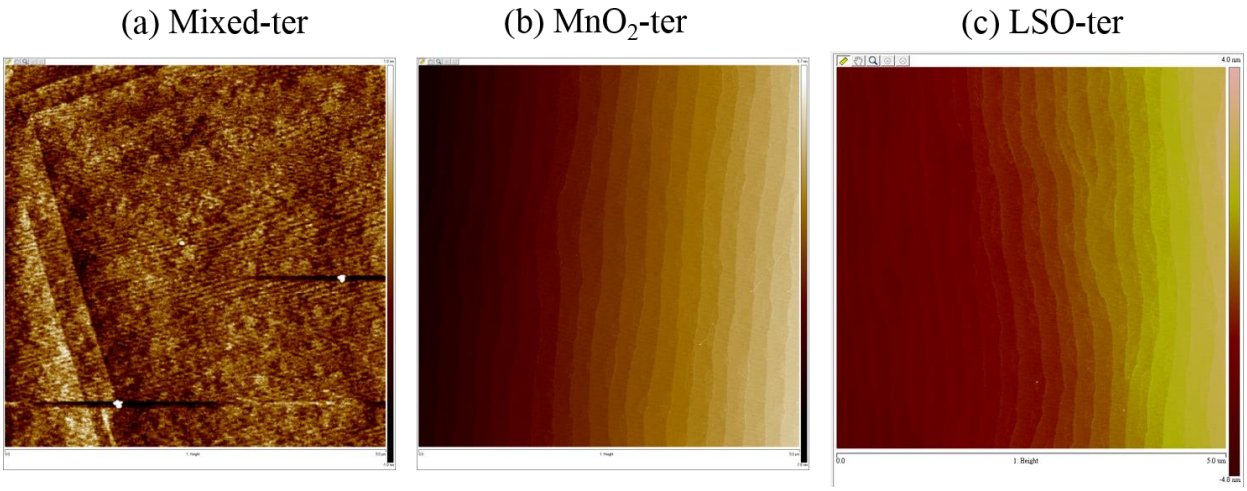

Fig. S1 Morphology of LSMO of various kinds: (a) mixed, (b) MnO_2, and (c) LSO terminations on a scanned area 5 μm x 5 μm.

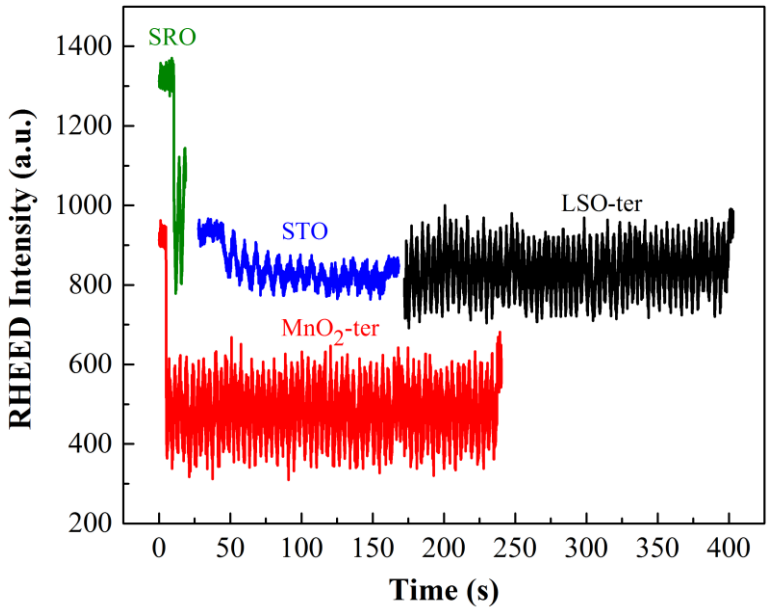

Fig. S2 RHEED intensity oscillations recorded during the epitaxial growth of LSMO termination layers of two kinds.

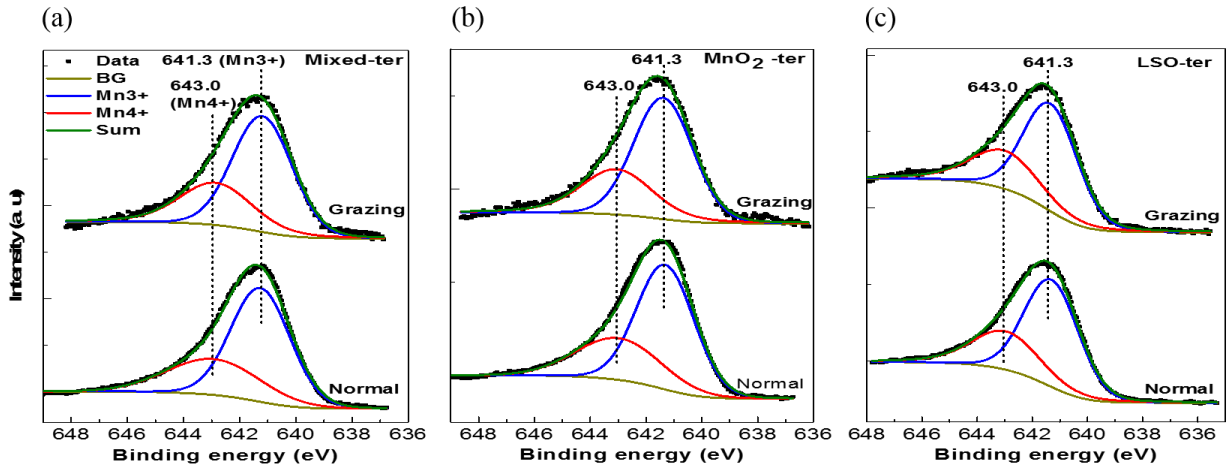

Fig. S3 Core-level photoelectron spectra of Mn 2p for (a) mixed, (b) MnO_2, and (c) LSO terminations recorded at photon energy 750 eV at grazing (top) and normal (bottom).

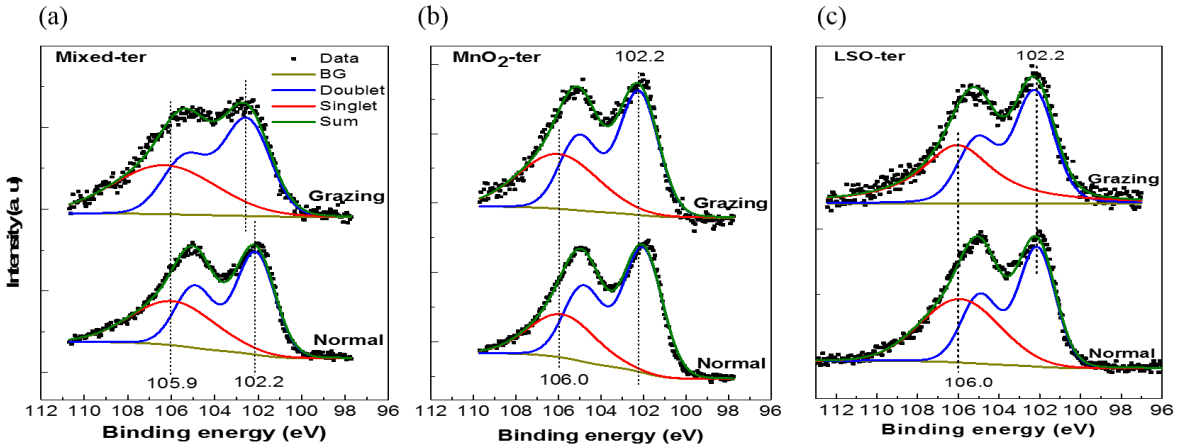

Fig. S4 Core-level photoelectron spectra of La 4d for (a) mixed, (b) MnO_2, and (c) LSO terminations recorded at photon energy 250 eV at grazing (top) and normal (bottom).

Sr 3d Ratio (Low BE : High BE)	Grazing	Normal
Mixed-ter	0.1 : 0.9	0.3 : 0.7
MnO_2-ter	0.2 : 0.8	0.4 : 0.6
LSO-ter	0 : 1	0.1 : 0.9

Table S1 Ratio between bulk and surface components of Sr 3d core level XPS at grazing and normal emission.

O 1s Ratio (Low BE : High BE)	Grazing	Normal
Mixed-ter	0.2 : 0.8	0.5 : 0.5
MnO_2-ter	0.2 : 0.8	0.6 : 0.4
LSO-ter	0.1 : 0.9	0.3 : 0.7

Table S2 Ratio between bulk and surface components of O 1s core level XPS at grazing and normal emission.

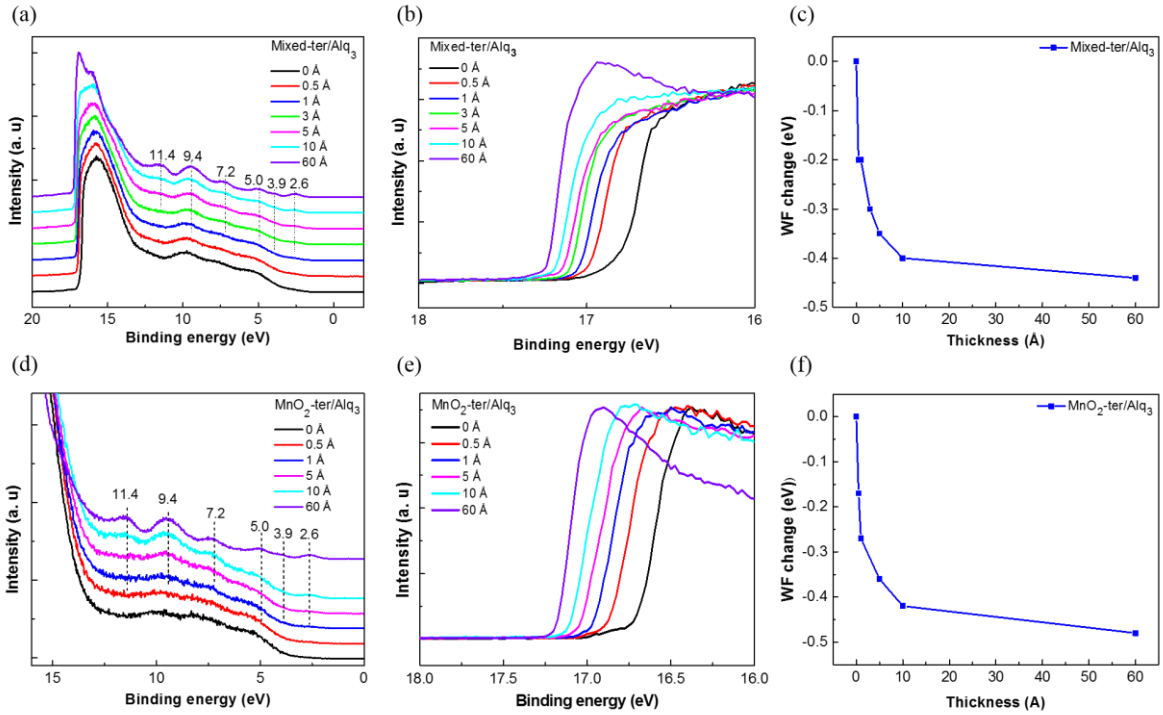

Fig. S5 Valence-band spectra, shift of secondary electron cut-off, and variation of work function with increasing Alq_3 thickness at mixed-ter/Alq_3 in (a), (b), and (c), respectively; and those at MnO_2-ter/Alq_3 interface in (d), (e), and (f), respectively.

References

[1] Q. Zhou, M. Dai, R. Wang, L. Jin, S. Zhu, L. Qian, Y. Wu, and J. Feng, Physica B: Condensed Matter **391**, 206 (2007).

[2] A. F. Monsen, F. Song, Z. S. Li, J. E. Boschker, T. Tybell, E. Wahlstrom, and J. W. Wells, Surface Science **606**, 1360 (2012).

[3] A. Thompson, X-ray Data Booklet, 3rd ed., Lawerence Berkeley National Laboratory (2009).